ELSEVIER

Catalysis Today 82 (2003) 105–118

CATALYSIS TODAY

www.elsevier.com/locate/cattod

Hydrodechlorination of chloroorganic compounds in ground water by palladium catalysts Part 1. Development of polymer-based catalysts and membrane reactor tests

Detlev Fritsch[a,*], Karsten Kuhr[a], Katrin Mackenzie[b], Frank-Dieter Kopinke[b]

[a] *Institute of Chemistry, GKSS Research Center, Max-Planck-Strasse 1, D-21502 Geesthacht, Germany*
[b] *Department of Remediation Research, UFZ-Environmental Research Center, Permoserstr. 15, D-04318 Leipzig, Germany*

Abstract

A polymer-based catalytic membrane reactor was developed and applied for hydrodechlorination of chlorobenzene as a model compound of ground and waste water contaminants. The catalytically active membrane consists of a non-porous, thin film (about 3–7 μm) of poly(dimethylsiloxane) (PDMS) loaded with nano-sized Pd clusters. They were built-in either directly or as nano-sized, supported catalysts. A composite membrane, consisting of porous poly(acrylonitrile) (PAN) support and a Pd-loaded thin PDMS film, was fabricated on a coating machine. Defect-free membrane envelopes of 0.1 m^2 were produced and fitted into a membrane test cell. Gaseous hydrogen as reductant for hydrodechlorination is fed from the membrane's back side directly to the catalyst, embedded in the PDMS layer. The chemical reactions at the Pd surface are accompanied by absorption of chlorobenzene from the water phase into the PDMS layer and desorption of benzene and HCl back to the water phase. The specific activity of supported catalysts decreased only slightly by PDMS incorporation, e.g., from 31 l/g(Pd) min for Pd/Fe on titania to 16 l/g(Pd) min for the same catalyst built-in a 7 μm thick supported PDMS membrane and measured in the membrane test cell. Directly built-in Pd clusters are less active and more difficult to prepare on a larger scale. Some catalyst deactivation was observed and may be balanced by development of more suited nano-sized supported catalysts.

Keywords: Hydrodechlorination; Membrane reactor; Pd catalyst; Catalysis in water; Polymer membrane

1. Introduction

Many halogenated hydrocarbons are hazardous compounds. Due to their lipophilic nature and persistence to biological degradation, accumulation in the environment may occur over the years. Despite their low water solubility, significant amounts are even found in ground water in some industrial areas. Biological degradation can be increased considerably by dehalogenation to the halogen-free hydrocarbons. Chemical treatment by catalytic hydrodehalogenation is a convenient and promising method for decontamination of organohalogen waste and contaminated water [1,2]. Palladium and palladium-based supported catalysts show a high activity towards hydrodehalogenation and can be used in the gas as well as in the liquid phase. To design the process as simple as possible, the liquid phase may be preferred and a three-phase reactor is applied. However, by treating waste water or contaminated ground water, other

* Corresponding author. Tel.: +49-4151-872463; fax:+49-4152-872444.
E-mail address: fritsch@gkss.de (D. Fritsch).

0920-5861/$ – see front matter © 2003 Elsevier B.V. All rights reserved.
doi:10.1016/S0920-5861(03)00208-6

compounds such as humic substances, heavy metals or sulfur compounds (other than sulfate) may poison the catalyst [3]. Moreover, in a traditional packed-bed reactor feeding of hydrogen to the catalyst via the water phase can be a bottle neck caused by its low solubility in water (0.8 mM at 20 °C and 100 kPa). These difficulties may be overcome by the use of a polymeric catalytic membrane reactor (PCMR). In this set-up a dense (pore-free) polymer membrane is doped with palladium, supports the catalyst and the reaction (hydrodehalogenation) takes place *inside* the polymer phase. The reactants and products must be able to diffuse to and from the catalyst's active sites with an acceptable rate. Therefore, a polymer with high diffusivity is strongly favored. In addition, hydrophobic polymers have high partition coefficients of the hydrophobic reactants from the water to the polymer phase and, therefore, concentrate the reactants in the polymer phase close to the catalyst. We have previously developed catalytically active membranes based on poly(dimethylsiloxane) (PDMS) and used them for gas-phase hydrogenation [4–7]. Using a simple method, catalytic activity is generated by loading the polymer film with metal salt precursors and subsequent reduction to form catalytically active nano-clusters of various noble metals [8,9]. Pure Pd is reported to have the highest activity for hydrodehalogenation [1]. However, catalyst-support interactions and doping of the catalyst or bimetallic catalyst may improve its activity, selectivity or stability. Supported catalysts have been incorporated inside PDMS membranes of 0.3–1 mm in thickness and tested successfully for hydrogenation of cyclopentadiene [10]. However, to provide high specific surface areas and short diffusion path lengths in the PCMR, thin-film composite membranes of thicknesses of about 1–10 μm are favored. Most of the commercial catalysts have to be ruled out, because their grain size usually does not fit into the required film thickness. Consequently, we selected nano-sized supports of titania and silica and prepared supported catalysts of pure Pd, Na_2O-doped Pd and Fe/Pd bimetallic catalysts. These catalysts were integrated in thin-film composite membranes. The activity of these supported catalysts and thick- as well as thin-film composite membranes with directly built-in Pd clusters was measured. A PCMR with a single membrane envelope (GKSS membrane envelope concept see, e.g., [11]) was constructed and applied in tests for selected thin-film composite membranes. Hydrodechlorination of chlorobenzene was selected as a representative test reaction to demonstrate the PCMR concept for treatment of ground and waste water.

2. Experimental

2.1. Chemicals

Anhydrous iron(II) acetate 95% (Aldrich) and palladium(II) acetate (Chempur) were used as catalyst precursors. All solvents were purchased from Merck as analytical grade. Titania P25® and the silica Aerosil Ox 50® were donated from Degussa-Huels and applied as nano-scale catalyst supports. The cross-linkable PDMS Dehesive® 930 or 942 from Wacker was used to prepare noble metal containing polymer films. In-house fabricated porous poly(acrylonitrile) (PAN) membranes with non-woven backing (about 14 nm pore size, 200 m^3_N/m^2 h bar N_2-flux) were used as thin-film supports. The polyether-*b*-amide Pebax® 4033 (Peba) was purchased from Atochem.

2.2. Preparation of supported catalysts

Na_2O-doped and pure Pd catalysts. The support was suspended in ethanol (about 10 ml/g) by the aid of an ultrasonic bath, and under stirring were added dropwise concentrated ethanolic solutions of NaOH and palladium acetate. After final addition stirring was continued for 30 min and it was evaporated to dryness. The residue was further dried at 105 °C and calcined in a muffle at 500 °C (10 °C/min) in air for 4 h.

Pd catalyst by ethanol reduction. 3.6 g titania was suspended in 500 ml ethanol using an ultrasonic bath. A solution of 0.42 g palladium acetate in 10 ml ethanol was added and the suspension refluxed for 30 min. The solvent was evaporated to dryness and the residue further dried at 70 °C.

Fe–Pd catalysts. 1.1 g iron(II) acetate was dissolved in 15 ml water and added dropwise under stirring to 5.7 g of catalyst support. The suspension was agitated for 5 min applying ultrasonic and evaporated. The residue was suspended in ethanol and evaporated to dryness. A solution of 0.63 g palladium(II) acetate in 10 ml ethanol (silica support) or 10 ml tetrahydro-

furan (THF, for titania support) was then added dropwise to the stirred, dry, pre-treated support. The suspension was agitated for 5 min in an ultrasonic bath, evaporated to dryness, dried at 120 °C, and calcined in a muffle at 500 °C (10 °C/min) in air for 4 h.

2.3. Membrane preparation

2.3.1. Membranes with nano-scale Pd catalysts

Thick films. 4 g Dehesive® (solvent-free) was dissolved in 10 g THF. The cross-linker and the catalyst were added (see Wacker data sheet) followed by a solution of 0.44 g palladium(II) acetate in 10 g THF. After short stirring, the homogeneous solution was poured onto a Teflon-coated glass plate. After evaporation of the solvent at RT over night, the polymer was further cross-linked at 70 °C for 4 h. The palladium acetate in the dark, homogeneous membrane was reduced by 1% $NaBH_4$ in methanol.

Thin-film composite membranes. 28.6 g solvent-free Dehesive® was dissolved over night in 173 g THF and subdivided into four samples. To each sample the required amount of cross-linker and catalyst were added followed by mixing with 0.76 g palladium(II) acetate dissolved in 60 g THF. Directly after mixing, the solution was dip-coated on the PAN support using a coating machine with subsequent cross-linking in a stream of hot air at 100 °C. Membrane thicknesses of 3–5 μm resulted in about 2 m^2 of composite membrane for each of the four samples. The membrane was reduced by 1% $NaBH_4$ in ethanol/water (1/1 by volume). A Pd content of 5% was calculated. The cluster size was estimated to 4 nm by XRD.

2.3.2. Membranes with supported catalysts

Solvent-free Dehesive® was used. Thick films were prepared from about 12% Dehesive® solutions, thin-film composite membranes from about 5% solutions. The supported catalyst was ball milled and sieved prior to use. THF, ethyl acetate (EA) or isooctane (*i*-C8) were used as solvents. A part of the desired solvent was taken to suspend the catalyst by the aid of an ultrasonic bath. With stirring the Dehesive® solution including the cross-linker and the catalyst was added, stirred for about 1 h and proceeded as described above for thick films and thin-film composites. The total Pd content of the films was between 1 and 1.5% according to about 30% of supported catalyst.

2.4. Methods

2.4.1. X-ray diffraction

XRD was measured and calculated as reported previously [9].

2.4.2. Scanning electron microscopy

A field emission scanning electron microscope (FESEM) (LEO Gemini VP 1550) was used. Au/Pd magnetron sputtered samples were analyzed by a secondary electron (SE) inline detector. Untreated samples were analyzed by the back scattering detector (BSD) at 2.2 Pa.

2.4.3. Catalytic activity and kinetic data

In a glass reactor equipped with gas outlet the catalyst (either polymer film or supported catalyst with about 2.5 mg Pd) was added to 300 ml water and the glass reactor was closed. At 25 °C H_2 gas was bubbled through the water for 1 h under magnetic stirring at 500–600 rpm to activate the catalyst. Film samples of dense membranes were activated prior to this procedure using 1% $NaBH_4$ in methanol. The films were washed and immediately mounted on a magnetically stirred rack. The gas outlet was closed and 2 ml of a methanolic solution containing 20 μl of chlorobenzene was added through a septum by a syringe to start the experiment. The gas phase was calculated to be 20 times the H_2 needed to reduce all chlorobenzene. From the head space 50 μl gas samples were taken and analyzed by GC every 3–5 or 10 min depending on the rate of the reaction. The gas chromatograph (GC 8000 Top Series, ThermoQuest with TCD and FID detectors) was operated isothermally at 150 °C (column: DB-1, 30 m, 0.53 mm ID (THK)). Various chlorobenzene/benzene/ethanol mixtures were used for calibration. Catalytic activity and kinetic data were also calculated from the experiments using the 0.1 m^2 membrane-envelope test apparatus.

2.4.4. Membrane reactor

The mounting of the membrane reactor is depicted in Fig. 1. A membrane envelope (GKSS system [11]) is installed in a single envelope test cell (3) with polypropylene spacers on the feed side to ensure turbulent flow. From the membrane's permeate side (11) H_2 is supplied and gas can be exchanged from the permeate side by a vacuum pump. A pH meter is connected

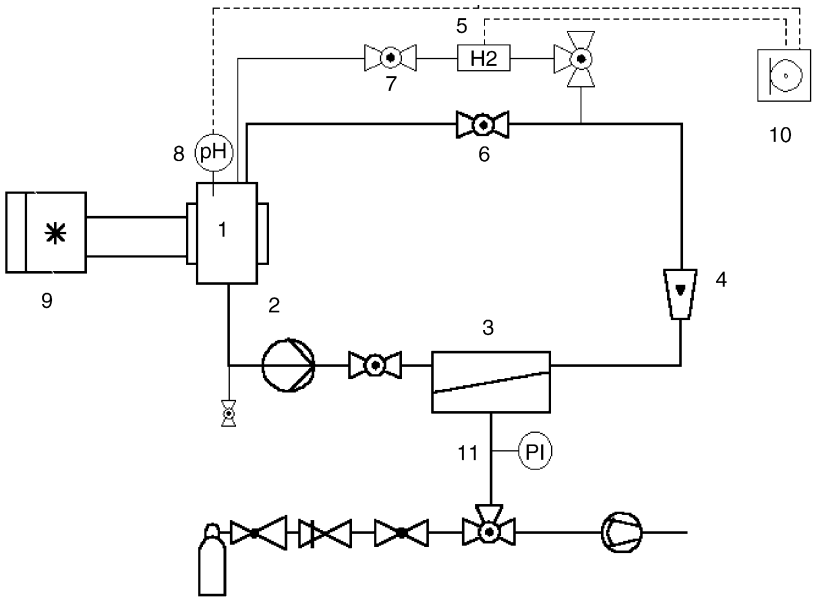

1 thermostated reaction vessel
2 pump (>400 L/h)
3 test cell for membrane envelope (1 m^2 membrane area)
4 flowmeter
5 hydrogen/temperature sensor
6 ball valve for flow regulation
7 ball valve for flow regulation
8 pH meter
9 thermostat
10 pen recorder (H_2, temperature, pH)
11 H_2-feeding with pressure sensor, gas supply, and vacuum pump

Fig. 1. Scheme of the membrane reactor set-up.

with a thermostated reaction vessel (1) to collect the reaction data online. A geared pump re-circulates the reaction mixture. The water flow is measured by a flow meter (4) and regulated using ball valves (6, 7). A combined H_2/temperature sensor is fitted into a by-pass. The concentration of H_2, temperature, and the pH are registered online (10). A typical test procedure is performed as follows: The defect-free membrane envelope ($P_{H_2} = 0.4\,m^3_N/m^2\,h\,bar$) is mounted in the test cell and the reaction vessel is charged with 6.3 l deionized water. The circulation pump is started and a flow of 400 l/h regulated. The thermostat is set to 21 °C. Chlorobenzene (PhCl, 0.31 g in 100 ml ethanol) is added and after 1 h of pumping, additional 0.3 g PhCl in 100 ml ethanol was added to balance the sorption of PhCl to the membrane. When the PhCl concentration remained constant, the run was started by evacuating the permeate side shortly and setting the H_2 pressure to 1 bar. The initial H_2 feed was 1.6 mg/h and a final H_2 concentration of 0.9 mg/l was detected in the solution after 3 h. For activity and kinetic measurement at the start additional H_2 was added by a frit to obtain immediately stable reaction conditions. Bearing the high Henry's law constants of PhCl and benzene (PhH) in mind ($K_H^{20\,°C} = 0.15$ for PhCl and $K_H^{20\,°C} = 0.25$ for PhH [12]), care has to be taken during sampling to avoid stripping of the contaminants. Samples were taken and analyzed.

3. Results and discussion

For the preparation of noble metal clusters inside polymer films, a simple method was developed previously [8,9]. However, it turned out, that on larger scale applications some adaptive difficulties occurred.

For this method, it is required to prepare a coating solution containing a polymer and the selected metal precursor, a suited metal salt. After film formation the solvent is evaporated and the film with the homogeneously distributed, amorphous metal precursor is reduced, e.g., by chemical or thermal treatment. In case of the PDMS Dehesive®, the cross-linker contains Si–H groups, known as a reducing agent. Therefore, reduction takes place already upon addition of the cross-linker to the coating solution. Metal-cluster formation starts and cross-linking is affected, if a considerable amount of Si–H groups is consumed by this side reaction. As a result, low temperatures, short mixing times, and fast casting or immediate coating are required. Using the PDMS Dehesive® and the described method, only batches of 2 m^2 could be produced with film thicknesses of 3–5 μm, cluster sizes of around 4 nm, and 5% Pd loading. An already pre-formed, supported catalyst would overcome this problem of up-scaling. Because film thicknesses of 1–5 μm are aspired, the appropriate grain size of the catalyst support is important. We selected commercial, nano-scale catalyst supports based on silica (Aerosil Ox 50) and titania (P25). Both supports have low primary particle sizes of about 25 nm (P25) and 40 nm (Aerosil Ox 50). The BET surfaces of $50 \pm 15\ m^2/g$ are relatively small. Some agglomeration of the particles is seen by SEM (not shown). Generally, the preparation of catalysts from these supports should be feasible following state-of-the-art procedures and a wide range of doped or bimetallic catalysts may result.

3.1. Catalyst preparation and characterization

Table 1 summarizes the composition and some properties of the compounded catalysts. With both supports three different types of catalysts, containing Na_2O, Pd or Fe, each around 5% were prepared: Na_2O-doped Pd (Na_2O/Pd), pure Pd (Pd), additionally pure Pd without calcination by ethanol reduction (Pd(EtOH)), and Pd–Fe bimetallic catalyst (Pd/Fe). Calcination in air at 500°C was generally carried out. In case of bimetallic catalyst, the impregnation with mixed ethanolic solutions of palladium acetate and iron acetate resulted in extremely poor activity of the calcined catalyst. Therefore, first an aqueous solution of iron acetate was applied, agitated in an ultrasonic bath followed by solvent evaporation. The residue was re-suspended in ethanol and again evaporated to dryness before the water-insoluble palladium acetate was applied for impregnation as ethanolic or THF solution. In the case of the calcined catalysts, Pd was detected as PdO by XRD. In case of the SiO_2 support, a minor amount of Pd(0) was found, too. TiO_2-based, pure Pd(0) catalyst, which were reduced by ethanol yielded exclusively Pd signals (all samples were stored for some weeks in air prior to XRD measurement). Iron was detected as $Fe_{21}O_{32}$ on silica catalyst (Pd/Fe–SiO_2), whereas with the similar titania catalyst (Pd/Fe–TiO_2) only traces of $Fe_{21}O_{32}$ could be determined (see Fig. 2).

The iron signal may be somewhat superimposed by the titania's rutile and anatase signals or some alloying may have occurred as well. Alloying may

Table 1
Composition and activity of supported catalysts

Notation	Support	Na_2O (%)	Pd (%)	Fe (%)	Pd (nm)[a]	PdO (nm)[a]	FeO_x (nm)[a]	Activity[b]
Na_2O/Pd–SiO_2	Aerosil Ox 50	4.7	5.0	–	24.9	18.7		13
Na_2O/Pd–TiO_2	TiO_2 (P25)	4.7	5.0	–	No	14.3		26
Pd(EtOH)–TiO_2	TiO_2 (P25)	–	5.3	–	12.7	No		12
Pd–TiO_2	TiO_2 (P25)	–	5.3	–	No	n.c.[c]		24
Pd/Fe–SiO_2	Aerosil Ox 50	–	4.7	5.6	n.c.	11.2	17	21
Pd/Fe–TiO_2	TiO_2 (P25)	–	4.7	5.6	No	8.1	n.c.	31
MERCK	Al_2O_3	–	5.0	–				8[d]

[a] Calculated from XRD signal.
[b] Initial specific activity of H_2-activated catalysts, for the hydrodechlorination of chlorobenzene given in [l(solution)/g(Pd) min]; $c_{0,PhCl} = 73$ ppm.
[c] Not calculated.
[d] From [15].

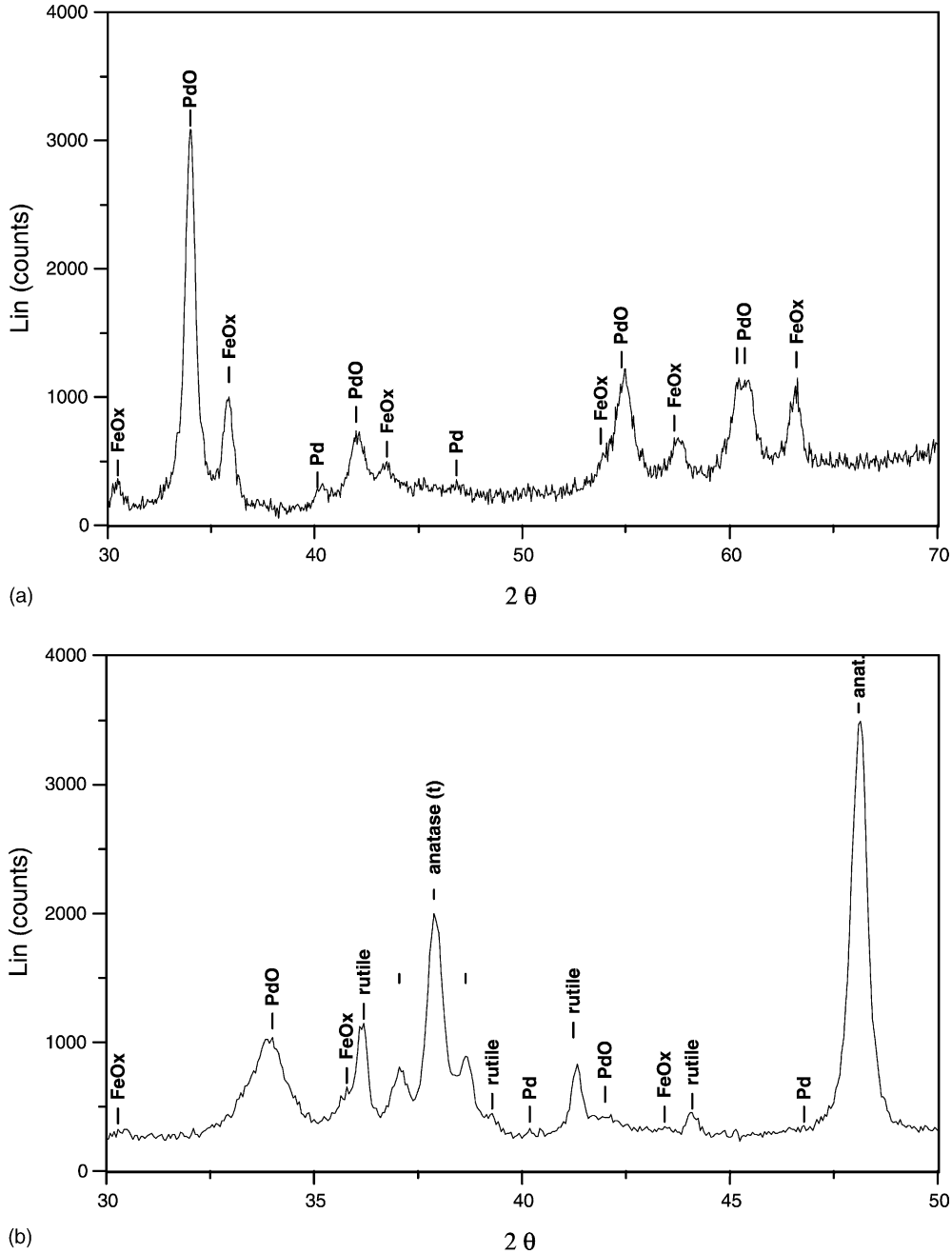

Fig. 2. XRD patterns of bimetallic catalysts. In the silica-supported catalyst (Pd/Fe–SiO_2) iron oxide is clearly detected (a), in a similar titania catalyst (Pd/Fe–TiO_2) only traces of iron oxide are found (b).

only shift the PdO signal slightly [13]. Cluster sizes could be calculated for some samples from XRD data by the Scherrer equation. The silica-based catalysts yielded 30–40% larger clusters than the titania-based catalysts. Bimetallic Pd/Fe-catalysts had the smallest cluster size within this series. Alloying of Pd with Fe could not be detected by XRD, definitely. Equimolar Fe–Pd supported onto graphite confirmed alloying of both metals only after high temperature reduction at 400 °C in flowing H_2 [13] and even under these conditions, separate zones of metallic iron remained. The XRD signal of Pd only shifted slightly to higher values from Pd (1 1 1) 40.15 2θ to Pd (1 1 1) 40.56 2θ. In the present work, the minor cluster size of PdO of the Fe-containing catalysts may result from higher dispersion of PdO caused by the preceding deposition of iron acetate during preparation. Table 1 shows that with decreasing cluster sizes the catalyst activity towards PhCl hydrodechlorination increases. Silica-based catalysts presented generally lower activities compared to titania-based catalysts. Na-doped titania-supported catalysts have similar activities compared to undoped catalysts (Na_2O/Pd–TiO_2: 26 l/g(Pd) min; Pd–TiO_2: 24 l/g(Pd) min). The Pd(EtOH)–TiO_2 catalyst, generated by direct adsorption of Pd clusters onto the support during slow reduction by boiling ethanol only gained half of the activity (12 l/g(Pd) min), whereby the size of the Pd clusters (12.7 nm (Pd) and 14.3 nm for Na_2O/Pd–TiO_2) are comparable. Summing up the results in Table 1 for supported catalysts, despite the different supports, additives and preparation procedures, their specific activities are similar. They are in the relatively narrow range of a factor 2.5. All prepared catalysts revealed superior activities in the hydrodechlorination of PhCl compared to the commercial Pd/Al_2O_3-catalyst (pulverized) from MERCK, which is in accordance to different particle sizes (nano-scale versus micro-scale).

3.2. Membrane preparation and characterization

The nano-scale supported catalysts (Pd/Fe–SiO_2 and Pd/Fe–TiO_2) were selected for the preparation of thin-film composite membranes. Because during calcination some agglomeration of particles had occurred, the catalysts were ground to restore the original particle size prior to application. Although the supported catalysts are nano-sized, utilizing the dip-coating procedure to produce thin-film composite membranes, sedimentation of the particles may take place which would result in non-uniform catalyst loading of the polymer membrane. Besides the size and porosity of the particles, their sedimentation rate will depend on the viscosity of the solution, mainly on the concentration of the polymer. The dispersion of the supported catalyst and the viscosity of the polymer solution depend further on the solvent, mainly on its polarity. We selected the non-polar isooctane and two polar solvents, THF and EA, for preparation of thin-film composite membranes. THF and EA have

Table 2
Preparation conditions and properties of the membrane catalysts

No.	Catalyst	Thickness[a] (μm)	Solvent	Composition of the coating solution		Final membrane catalyst	
				PDMS (%)	Catalyst (%)	Support catalyst (%)	Pd (%)
1	Pd/Fe–TiO_2 supported catalyst	–	–	–	–	–	4.7
2	Pd/Fe–SiO_2 supported catalyst	–	–	–	–	–	4.7
3	Pd/Peba	20	DMAc	4.0 (Peba)	0.7[b]	None	7.7
4	Pd/PDMS	62	THF	14.0	1.6[b]	None	5.0
5	Pd/Fe–SiO_2	200	Isooctane	11.5	4.9	30	1.4
6	Pd/PDMS	4	THF	10.2	1.1[b]	None	5.0
7	Pd/Fe–SiO_2	11	Isooctane	6.8	2.9	30	1.4
8	Pd/Fe–SiO_2	5	Isooctane	6.0	1.7	22	1.0
9	Pd/Fe–SiO_2	9	EA	6.8	2.0	22	1.0
10	Pd/Fe–SiO_2	30	THF	6.8	2.0	22	1.0
11	Pd/Fe–TiO_2	7	Isooctane	6.0	2.5	30	1.4

[a] All membranes were defect-free as tested by gas selectivity of $\alpha(O_2/N_2) > 2.1$.
[b] Palladium(II) acetate.

very similar polarities, however, EA is the better solvent for PDMS. From all three solvents defect-free films with catalyst loading up to 30% could be prepared by dip-coating on a coating machine suited for continuous coating in the range of 50 m^2. The quality of the films was checked by gas-selectivity measurement and SEM microscopy. The measured gas selectivities of $\alpha(O_2/N_2) > 2.1$ indicate, that all membranes were defect-free.

Table 2 summarizes the composition of the coating solutions and the catalyst content of the final thin-film composite membranes. Film thicknesses obtained were between 4 and about 10 μm. When supported catalysts were added to the PDMS coating solution, thicker membranes resulted compared to membranes free of supported catalysts. In the case of sample No. 10 with 30% supported catalyst in the PDMS film, the THF solution was highly viscous during coating and the highest thickness of 30 μm was obtained. Total Pd contents of 5% (No. 6 with directly built-in Pd clusters) and 1–1.4% for implemented supported catalysts were achieved.

In Fig. 3 some SEM micrographs are presented. Depending on the quality of grinding, somewhat rough surfaces were obtained as can be seen in Fig. 3a and d. In the back scattering mode (Fig. 3c) some insight in the uppermost membrane surface is given. As a side effect, surface roughness may increase the turbulent flow and, therefore, contribute to reduce a possible polarization of the boundary layer during the reaction. Inside the membranes agglomerated supported catalyst particles are well distributed throughout the

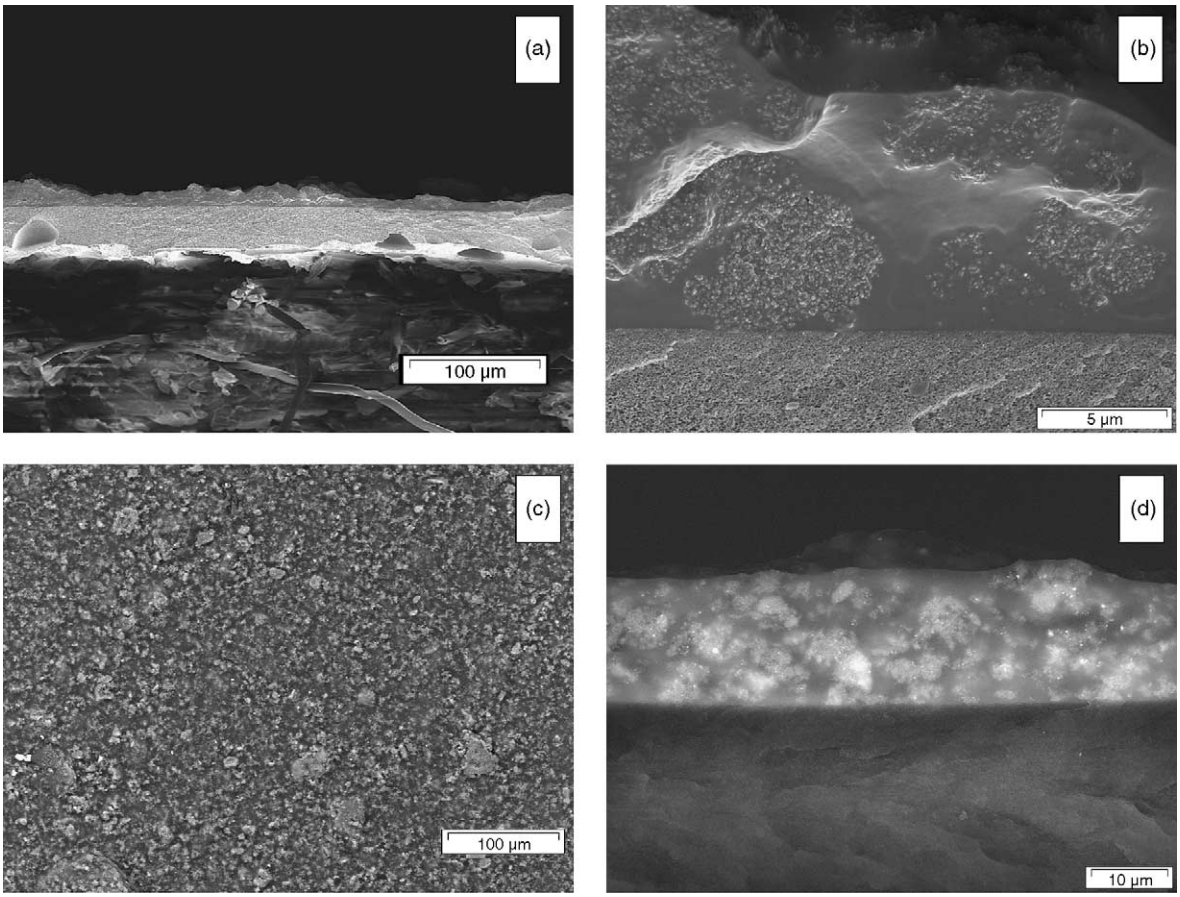

Fig. 3. SEM micrographs from thin-film composite membranes. Cross-section membrane No. 9 of Table 2 in low magnification (a) and high magnification (b) by SE detector. Membrane No. 10 of Table 2 in BSD mode, surface (c) and cross-section (d).

Table 3
Properties and catalytic features of supported catalysts and membrane-incorporated catalysts

No.[a]	Shortcut	Solvent[b]	Type	Thickness[c] (μm)	Pd[d] (nm)	Pd[e] (%)	Activity (l/g(Pd) min)
1	Pd/Fe–TiO_2	–	Supported catalyst	–	8	4.7	31
2	Pd/Fe–SiO_2	–	Supported catalyst	–	11	4.7	21
3	Pd//Peba	DMAc	Pd/polymer	50	∼5	7.7	0.7
4	Pd//PDMS	THF	Pd/polymer	62	∼5	5.0	2.3
5	Pd/Fe–SiO_2//PDMS	*i*-C8	Supported catalyst/polymer	200	11	1.4	1.3
6	Pd//PDMS/envelope	THF	Pd/polymer	4	∼5	5.0	1.9
7	Comp. SiO_2	*i*-C8	Supported catalyst/polymer	11	11	0.5	2.6
8	Comp. SiO_2	*i*-C8	Supported catalyst/polymer	5	11	1.0	1.9
9	Comp. SiO_2	EA	Supported catalyst/polymer	9	11	1.0	6.7
10	Comp. SiO_2	THF	Supported catalyst/polymer	30	11	1.0	3.9
11	Comp. TiO_2	*i*-C8	Supported catalyst/polymer	7	8	1.4	13
12	Comp. TiO_2/envelope 1. run	*i*-C8	Supported catalyst/polymer	7	8	1.4	16
13	Comp. TiO_2/envelope 2. run	*i*-C8	Supported catalyst/polymer	7	8	1.4	9.7
14	Comp. TiO_2/envelope 6. run	*i*-C8	Supported catalyst/polymer	7	8	1.4	4.1

[a] Numbers 1–11 according to Table 2.
[b] Solvents for membrane preparation: DMAc: dimethyl acetamide, THF: tetrahydrofuran, *i*-C8: isooctane, EA: ethyl acetate.
[c] Thickness of pore-free film either free-standing or thin-film composite. Measured by calculation from gas flux, SEM or micrometer.
[d] Cluster size by XRD.
[e] Pd content in dense films or supported catalysts.

active membrane layer. The agglomerated nano-sized particles can be seen in Fig. 3b—SE detector and 3d—BSD detector—visualizing the contrast of catalyst support/Pd and PDMS layer. From membrane types (see Tables 2 and 3) 6 (Pd/PDMS) and 11 (Pd/Fe–TiO_2), membrane envelopes of 1010 cm^2 area were produced and tested in the PhCl hydrodechlorination using the membrane reactor (see exp. part for details).

3.3. Activity and kinetic data

Table 3 summarizes the properties of supported catalysts, thick, free-standing catalytically active polymer membranes from Peba and PDMS, various thin-film composite membranes with directly incorporate Pd clusters, silica-supported catalysts prepared with different solvents, and similar titania-supported catalysts. Fig. 4 displays typical graphs from experimental data for calculation of catalyst activities and kinetic constant.

As can be seen in Fig. 4a after a short induction period, a constant decomposition rate of PhCl up to at least 60% degree of conversion appears. The reaction order is between zero and one with respect to PhCl. From the slope was calculated the half-life of PhCl and the catalyst activity according to Eq. (1). With supported catalysts in the same plot (not shown) the linearity between 40 and 50% conversion leveled off asymptotic to 0%. The same data as in Fig. 4a are recalculated and plotted in Fig. 4b as $\ln(C_t/C_0)$ by time. A fairly good straight line was observed after the induction period and a pseudo-first-order kinetic may be assumed. The kinetic constant of the titania-supported catalyst (1, Pd/Fe–TiO_2) diminished by means of membrane incorporation from $k = 5.7 \times 10^{-3}\,s^{-1}$ to $k = 8.5 \times 10^{-4}\,s^{-1}$ (11, comp. TiO_2). The initial kinetic constant further decreased to about half of this value in envelope configuration performing the tests in the membrane reactor (set-up see Fig. 1, these kinetic data depends on the reactor properties). Literature data on kinetics of PhCl hydrodechlorination in water are rare. Murena and Gioia [14] found also pseudo-first-order kinetics for this reaction and reported $k_{ClB_z} = 7.0 \times 10^{-4}\,s^{-1}$ at 30 °C for a commercial 5% Pd on carbon catalyst.

Various types of supported catalysts have been prepared in our study. Main features are the polymer encapsulation and the different thicknesses of the final membranes. As the characteristic parameter of the

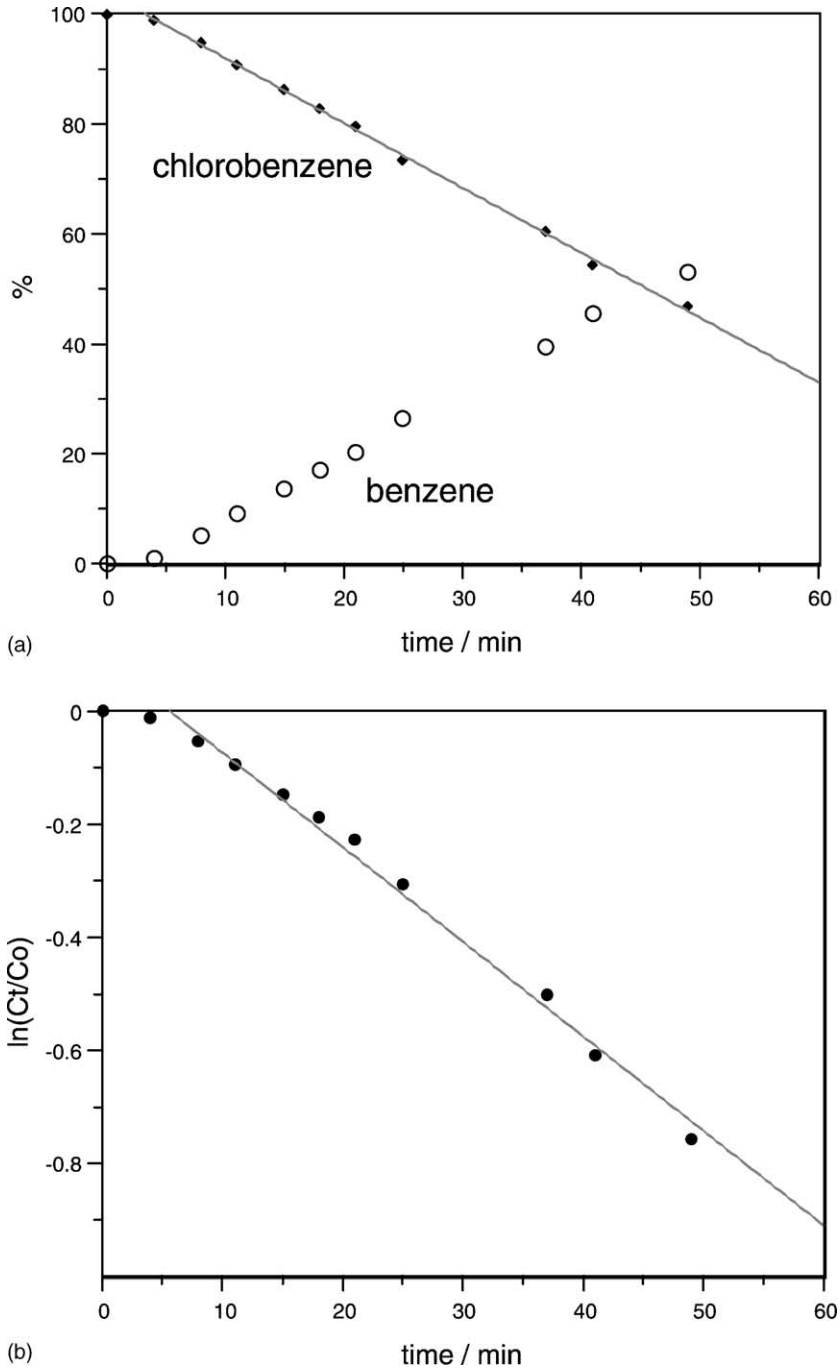

Fig. 4. Hydrodechlorination of chlorobenzene with membrane No. 10, Table 3: conversion versus reaction time (a) and semi-logarithmic plot according to a first-order kinetics (b).

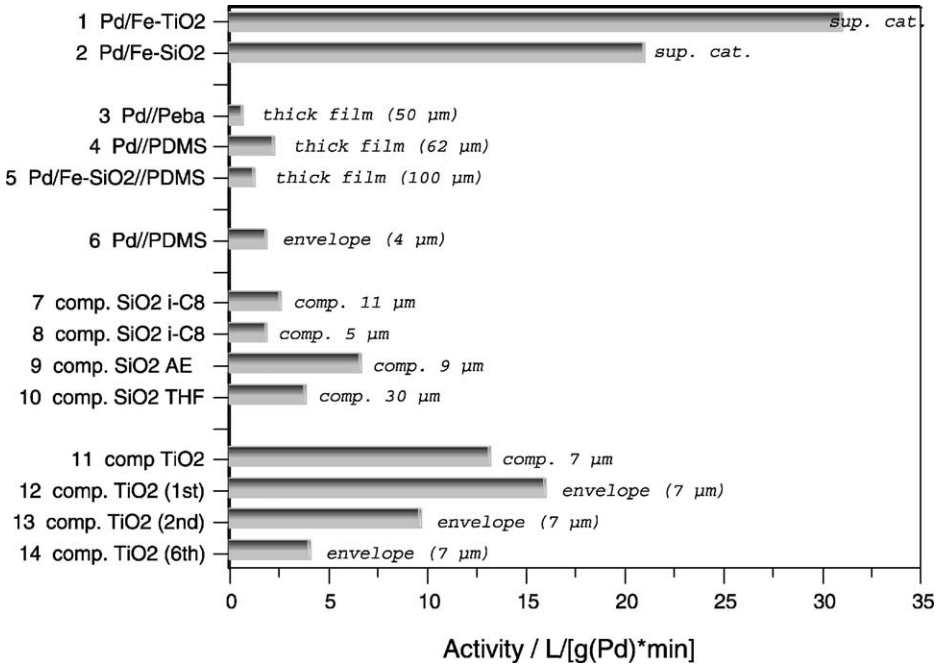

Fig. 5. Catalyst activities for supported catalysts and membrane catalysts. Nos. 12–14 are data from the membrane reactor of the first, second and sixth reaction run. Numbering according to Tables 2 and 3.

catalyst we use its activity defined as

$$A = \text{reaction volume (l)}/[\text{mass Pd(g)} \times \text{half-life (min)}] \quad (1)$$

Therefore, the efficiency of the decomposition of PhCl in water correlates directly with this activity.

Fig. 5 graphically presents activities for supported catalysts (1, 2), thick films containing similar Pd-cluster sizes from Peba (3) and PDMS (4), and built-in supported catalyst (5). Also, thin-film composite membranes from directly built-in Pd clusters (6), silica-supported catalysts (7–10), and titania-supported catalysts (11–14). Activities from catalytically active membranes (6, 12–14) are calculated from data obtained in the membrane reactor test cell fitted with membrane envelopes. In all cases the activity diminishes with encapsulation of the Pd-catalyst into the polymers. Comparing activities of thick films with matchable Pd-cluster size and thickness but made from different polymers, Peba-based Pd clusters are less active by about a factor of 3 (Fig. 4 and Table 3). The main difference between Peba and PDMS is their diffusivity. For instance, the apparent diffusion coefficient of H_2 is about one order of magnitude lower in case of Peba (Table 4). A similar dependence is reasonable for the other reactants.

The thick PDMS film loaded with supported catalyst (5, Table 3) is less active by about a factor of 2, yet it is also about three times as thick as the PDMS film with directly built-in Pd clusters ($4 = 62\,\mu m$ versus $5 = 200\,\mu m$). However, a direct comparison of activities between directly built-in Pd clusters and supported Pd catalyst is not conclusive with the available data. The larger thickness may prevent some Pd deeply inside the polymer matrix from reaction due

Table 4
Apparent diffusion coefficients of reactants in polymers and water

Material	Reactant	D_a ($\times 10^{-6}$ cm^2/s)	Source
Peba	H_2	4.4	GKSS, Pebax® 4033
PDMS	H_2	68	GKSS, Dehesive®
PDMS	Benzene	2.7	[15]
PDMS	Chlorobenzene	2.2	[15]
Water	Benzene	10	[15] from CRC Handbook

to the long diffusion path. The thick film 5 is made from the same supported catalyst and polymer as the thin-film composites 7–10. All the thin film catalytic membranes are more active than the thick film ones. We contribute this to effects of outer and inner transport resistances. As an example, catalyst 9 has an outer specific surface area of 111 cm^2/mg Pd in comparison to catalyst 5 with only 7.4 cm^2/mg Pd. Within the series of silica-supported catalyst the solvent for preparing the thin-film composite membranes had some effect. Best solvent was EA, probably due to adapted polarity between silica and PDMS to give well dispersed suspensions. Titania-supported catalysts could be well prepared from isooctane. The composite membranes preserved the higher activity of the supported catalysts (compare: 1 and 2 with 9 and 11). The high activity of 13 l/g(Pd) min was also realized with the envelope in the test apparatus, thus proofing the favorable design of the test cell (see 11 and 12, Table 3). However, after several runs the activity decreased by a factor of 4. This reduced activity of the 'altered' support-based catalyst is even higher than that of 'fresh' directly built-in Pd clusters (6 see Table 3).

4. Qualitative discussion of results

Mass transport is the main limitation with fast, catalytic reactions. For PhCl hydrodechlorination in the liquid phase, a three-phase system has to be considered: gaseous H_2, water with dissolved PhCl and benzene, and the solid Pd-catalyst (including the polymer phase).

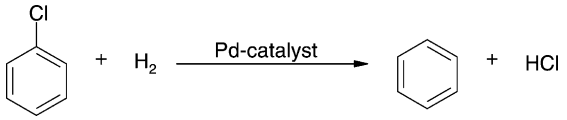

Fig. 7. Scheme of chlorobenzene reduction.

Fig. 6 sketches the feeding of educts and products to and from the membrane-based catalyst. Considering the stoichiometry of the PhCl hydrodechlorination (Fig. 7) molar amounts of each reactant have to be transported. To the catalyst: from aqueous phase the PhCl, from the gas phase the H_2, and back from the catalyst to the aqueous phase benzene and HCl (also some diffusion to the gas phase has to be considered). A special benefit of this membrane system is that the transport of H_2 to the catalyst is decoupled from its limited solubility in water. The delivery from the gas phase directly to the Pd-catalyst via the PDMS phase is fast ($D_{a\,H_2} = 68 \times 10^{-6}$ cm^2/s, Table 4; typical flow of $H_2 = 0.4\,m^3_N/m^2$ h bar). In time-lag experiments it was observed that the break-through of H_2 is detected only after saturation of the Pd clusters, as can be seen by the drastical decrease in the apparent diffusion coefficient (D_a) of H_2 in Pd-cluster loaded and unloaded

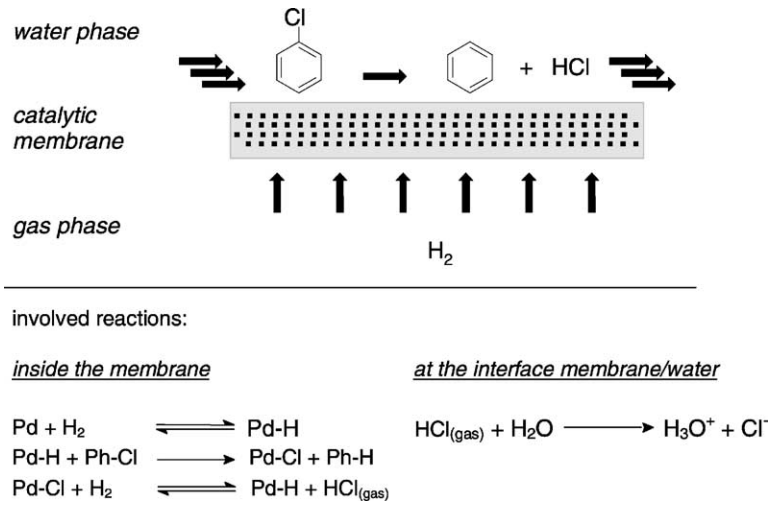

Fig. 6. Schematic presentation of the educts and products transport to and from the catalyst.

films [8,9]. After reaching sorption equilibrium, the H_2 flux through the membrane is not markedly affected by the presence of the Pd-catalyst. By setting different pressures the H_2-flux to the Pd-catalyst can be regulated easily. The apparent diffusion coefficients of PhH and PhCl in PDMS are only about four times lower than in water (Table 4). This effect has to be compared with pore diffusion in pelletized supported catalysts, as they are usually applied in fixed-bed reactors. The length of that diffusion path is in the order of some 10^3 μm. According to $t_{diff} = L^2_{path}/D_a$ the lower value of D_a in PDMS may be compensated for by the shorter diffusion path length in our membranes. Furthermore, the lower D_a may be counterbalanced by the enrichment of the PhCl from water into the PDMS phase (factor of about 400 [15]). Köhler [15] reports data on the kinetics of desorption of PhH and PhCl from PDMS into the gas phase. The half-life of benzene desorption from a 400 μm membrane was in the order of 100 s. Extrapolating these data to a film thickness of 5 μm according to $t_{1/2} \sim$(film thickness)^2 one obtains extremely short half-lives in the order of $t_{1/2} \ll 1$ s for the intra-membrane diffusion. Beside the geometric parameters and diffusivities mass fluxes depend also on the driving forces as can be expressed as gradient of reactant activities from inside to outside the membrane. The presence of the product benzene in the water phase will reduce its desorption rate. In case of the product HCl the dissociation process is involved. Inside the membrane HCl is formed at the catalysts surface and diffuses without a solvation shell to the membrane/water interface. Upon contact with bulk water, dissolution and immediate dissociation occurs. Independent pervaporation experiments of phenol in diluted aqueous hydrochloric acid with Peba or PDMS membranes teaches, that the reverse transport of HCl, once dissolved in water, through the PDMS membrane does not take place. Not even traces of acid were detected in the permeate [16]. Therefore, the driving force for HCl desorption from the membrane into the water phase is always high. So far, we discussed the transport resistance of the PDMS (polymer) to the overall reaction. How is the situation at the catalyst surface? Marked sorption with high binding constants for PhCl and PhH at the catalyst are not expected due to the hydrophobic environment inside the polymer matrix. Chlorine (or chloride), however, as an intermediate product of the hydrodechlorination is known to poison the catalyst [1,17–19]. As a result of a theoretical study on Pd (1 1 1) surfaces [19] it was concluded, that even on chlorine-saturated surfaces hydrogen adsorption is possible. Removing of chlorine may, therefore, be possible according to

$$\text{Pd–Cl} + 2[\text{H}] \leftrightarrow \text{Pd–H} + \text{HCl} \quad (2)$$

A slow decrease of pH during washing of used membranes in water supports this hypothesis. For hydrodechlorination of CFC 114a in the gas phase at 150 °C on a Pd-catalyst it was found that the rate determining step is the adsorption of CFC 114a while the catalyst surface is covered with chlorine that is in equilibrium with H_2 and HCl in the gas phase [20]. For hydrodechlorination at RT the equilibrium is expected to shift to the left side (Pd–Cl), explaining the slow release of HCl from the catalyst. As a result, this may be the rate determining step at RT after some time of reaction. More active catalysts for hydrodechlorination in water are known to be more sensitive to chlorine poisoning (see [1]). Comparing a typical batch reactor to a fixed-bed reactor an improvement was detected [21] and attributed to a generally lower HCl presence at the catalyst due to the continuous process. This advantage is also valid for the PCMR concept but up to now it is difficult to compare the data directly.

5. Conclusion

A PCMR concept was developed with the advantage of direct feeding of H_2 to the catalyst. The catalyst is enclosed completely by a continuous PDMS film and applied as a thin-film composite membrane on a porous supporting membrane. Defect-free membrane envelopes of 0.1 m^2 were fabricated and tested in a single envelope membrane test cell with H_2 feed from the membrane's back side. Catalytically active thin-film composite membranes from directly built-in Pd clusters and nano-sized, supported Pd-catalysts were produced and their activity was measured in a test apparatus and a membrane reactor. Membrane fabrication on large, continuous scale was demonstrated. Initial catalyst activities for hydrodechlorination of chlorobenzene were measured. The most active supported catalyst has a specific activity of 31 l/g(Pd) min. This value decreased by only a factor of 2 by fitting

the catalyst into thin-film composite membranes. Both values are quite acceptable. Membrane catalysts with directly built-in Pd clusters are by an order of magnitude less active. In addition, those membranes also can hardly be produced continuously on a larger scale than 2 m^2. Some catalyst deactivation was noted after several reaction runs. Possibly, this can be attributed to partial poisoning by adsorbed chlorine. It is suggested, that improvement of supported catalysts may increase the chlorine tolerance of the catalysts and, therefore, of the whole process. However, approaching the task of real ground water treatment, additional care must be taken for generation of sulfide by microbial sulfate reduction [22]. Although the membrane-based catalyst is safely protected from contact to dissolved ions by the polymer shield, non-ionic components such as H_2S can easily penetrate the membrane and poison the catalyst. In that case, the PDMS encapsulation may be a disadvantage, because rigorous catalyst reactivation procedures are restricted by the sensitivity of the membrane to harsh treatment.

Acknowledgements

This work was funded in part by the German Federal Ministry of Education and Research (BMBF 02WT9949/9 and 02WT9940/9) as a contribution to the interconnected project “Remediation Research in Regionally Contaminated Aquifers” (SAFIRA). Petra Merten is thanked for technical assistance and Dr. Michael Oehring for XRD measurement, cluster size calculation, and discussion.

References

[1] F.J. Urbano, J.M. Marinas, J. Mol. Catal. A 173 (2001) 329.
[2] K. Pirkanniemi, M. Sillanpää, Chemosphere 48 (2002) 1047.
[3] F.-D. Kopinke, R. Köhler, K. Mackenzie, H. Borsdorf, C. Schüth, Grundwasser 3 (2002) 140.
[4] J. Theis, D. Fritsch, F. Keil, in: Proceedings of the ESF, Network Catalytic Membrane Reactors—Final Workshop: Applications and Future Possibilities of Catalytic Membrane Reactors, Turnhout, Belgium, October 16–17, 1997, p. 35.
[5] J. Theis, Entwicklung und Anwendung von katalytischen Polymermembranen, Thesis, Hamburg-Harburg, 2000.
[6] K. Mackenzie, R. Köhler, H. Weiss, F.-D. Kopinke, in: G.B. Wickramanayake, A.R. Gavaskar, A.S.C. Chen (Eds.), Chemical Oxidation and Reactive Barriers: Remediation of Chlorinated and Recalcitrant Compounds, Batelle Press, Columbus, Richland, 2000, pp. 331–338.
[7] F.-D. Kopinke, R. Köhler, K. Mackenzie, H. Weiss, C. Schüth, Wasserwirtschaft Wassertechnik Abwassertechnik 7 (2000) 58.
[8] D. Fritsch, K.-V. Peinemann, J. Membr. Sci. 99 (1995) 29.
[9] L. Tröger, H. Hünnefeld, S. Nunes, M. Oehring, D. Fritsch, J. Phys. Chem. B 101 (1997) 1279.
[10] V.M. Gryaznov, V.S. Smirnov, V.M. Vdovin, M.M. Ermilova, L.D. Gogua, N.A. Pritula, G.K. Fedorova, US Patent 4,394,294, July 19, 1983.
[11] V. Nitsche, K. Ohlrogge, K. Stürken, Chem. Eng. Technol. 21 (1998) 925.
[12] J. Staudinger, P.V. Roberts, Crit. Rev. Environ. Sci. Technol. 26 (1996) 205.
[13] R. Wunder, J. Phillips, J. Phys. Chem. 98 (1994) 12329.
[14] F. Murena, F. Gioia, Cat. Today 75 (2002) 57.
[15] R. Köhler, Elektrochemische und katalytische Dechlorierung von Chlorkohlenwasserstoffen im Grundwasser, Thesis, Magdeburg, 1999, UFZ-Bericht Nr. 5/2000. ISSN 0948-9452.
[16] G. Bengtson, Unpublished results.
[17] M.A. Aramendía, V. Boráu, I.M. García, C. Jiménez, F. Lafont, A. Marinas, J.M. Marinas, F.J. Urbano, J. Mol. Catal. A 184 (2002) 237.
[18] S. Rajagopal, A.F. Spatola, J. Org. Chem. 60 (1995) 1347.
[19] P.A. Gravil, H. Toulhoat, Surf. Sci. 430 (1999) 176.
[20] F.H. Ribeiro, C.A. Gerken, G.A. Somorjai, C.S. Kellner, G.W. Coulston, L.E. Manzer, L. Abrams, Catal. Lett. 45 (1997) 149.
[21] P. Forni, L. Prati, M. Rossi, Appl. Catal. B 14 (1997) 49.
[22] N.E. Korte, J.L. Zutman, R.M. Schlosser, L. Liang, B. Gu, Q. Fernando, Waste Manage. 20 (2000) 687.